AIP Journal of Applied Physics

Nonlinear frequency-dependent effects in the dc magnetization of uniaxial magnetic nanoparticles in superimposed strong alternating current and direct current fields

Nijun Wei, Declan Byrne, William T. Coffey, Yuri P. Kalmykov, and Serguey V. Titov

Citation: Journal of Applied Physics **116**, 173903 (2014); doi: 10.1063/1.4900618
View online: http://dx.doi.org/10.1063/1.4900618
View Table of Contents: http://scitation.aip.org/content/aip/journal/jap/116/17?ver=pdfcov
Published by the AIP Publishing

Nonlinear frequency-dependent effects in the dc magnetization of uniaxial magnetic nanoparticles in superimposed strong alternating current and direct current fields

Nijun Wei,[1] Declan Byrne,[2] William T. Coffey,[1] Yuri P. Kalmykov,[3] and Serguey V. Titov[4]
[1]*Department of Electronic and Electrical Engineering, Trinity College, Dublin 2, Ireland*
[2]*School of Physics, University College Dublin, Belfield, Dublin 4, Ireland*
[3]*Laboratoire de Mathématiques et Physique (LAMPS), Université de Perpignan Via Domitia, F-66860 Perpignan, France*
[4]*Kotel'nikov Institute of Radio Engineering and Electronics of the Russian Academy of Sciences, Vvedenskii Square 1, Fryazino, Moscow Region 141120, Russia*

(Received 19 September 2014; accepted 17 October 2014; published online 3 November 2014)

The dc component of the magnetization of noninteracting fine magnetic particles possessing simple uniaxial anisotropy and subjected to strong ac and dc bias magnetic fields is calculated via the magnetic Langevin equation. In the presence of an ac driving field, the dc component of the magnetization of uniaxial particles alters drastically leading to new nonlinear effects; in particular, it becomes frequency-dependent. In axial symmetry, where the strong ac field is parallel to the easy axis of a particle, two distinct dispersion regions in the dc magnetization at low and mid-frequencies emerge, corresponding to longitudinal overbarrier and intrawell relaxation modes. Such frequency-dependent behavior allows one to estimate the magnetization reversal time via the half-width of the low-frequency dispersion band. Otherwise, by applying the strong ac field at an angle to the easy axis of a particle so breaking the axial symmetry, a third high-frequency nonlinear resonant dispersion in the dc component of the magnetization appears accompanied by parametric resonance behavior due to excitation of transverse modes with frequencies close to the precession frequency. © *2014 AIP Publishing LLC*. [http://dx.doi.org/10.1063/1.4900618]

I. INTRODUCTION

A fine ferromagnetic particle is characterized by an internal magnetocrystalline anisotropy potential with several local states of equilibrium and potential barriers between them depending on the size of the particle. If the particles are small ($\sim$10 nm) so that the barriers are relatively low, the magnetization vector $\mathbf{M}$ may cross over from one potential well to another and vice versa due to thermal agitation with a relaxation time, which exponentially depends on the volume of a particle. The ensuing thermal instability of the magnetization of fine particles results in superparamagnetism and in magnetic aftereffect. The thermal fluctuations and relaxation of the magnetization of such particles play a central role in information storage, rock magnetism, magnetic hyperthermia, etc.,[1,2] while due to the large magnitude of their magnetic dipole moment ($\sim 10^4$–10^5 μ_B), the Zeeman energy is relatively large even in moderate external magnetic fields. Hence we expect that their magnetization dynamics will exhibit a pronounced field and frequency dependence,[3] which is significant because the nonlinear response of fine particles driven by a strong ac field occurs in diverse physical applications. These include nonlinear dynamic susceptibilities and field induced birefringence,[3–6] nonlinear stochastic resonance,[7] dynamic hysteresis,[8–10] and microwave field effects.[11,12]

The calculation of the nonlinear magnetic response of nanomagnets in the presence of thermal agitation originating in a heat bath usually commences with the magnetic Langevin equation. This is Gilbert's (or the Landau-Lifshitz) equation augmented by a random magnetic field $\mathbf{h}(t)$ with Gaussian white noise properties, accounting for the thermal fluctuations of the magnetization $\mathbf{M}(t)$ of an individual particle,[13] viz.,

$$\dot{\mathbf{M}}(t) = \gamma[\mathbf{M}(t) \times [-\partial V_{\mathbf{M}}(t) - \eta\dot{\mathbf{M}}(t) + \mathbf{h}(t)]]. \quad (1)$$

Here, γ is the gyromagnetic ratio, η is the damping parameter, and V is the free energy per unit volume comprising the *non-separable* Hamiltonian of the magnetic anisotropy and Zeeman energy densities, and M_S is the saturation magnetization, assumed constant so that the only variable is the orientation of $\mathbf{M} = M_S\mathbf{u}$, which is specified by the polar and azimuthal angles ϑ and φ of the spherical polar coordinate system. The stochastic differential Eq. (1) is then used to derive the accompanying Fokker-Planck equation (FPE) governing the time evolution of the probability density function $W(\mathbf{u}, t)$ of magnetization orientations on the surface of a sphere of constant radius M_S ($\mathbf{u}$ is a unit vector along $\mathbf{M}$), and the relevant FPE is[13]

$$2\tau_N \frac{\partial W}{\partial t} = \nabla^2 W + \frac{\beta}{\alpha}(\mathbf{u} \cdot [\nabla V \times \nabla W]) + \beta(\nabla \cdot W \nabla V). \quad (2)$$

Here, $\nabla = \partial/\partial\mathbf{u}$ is the gradient operator on the unit sphere, $\alpha = \gamma\eta M_S$ is the dimensionless damping constant, $\tau_N = \tau_0(\alpha + \alpha^{-1})$ is the characteristic free diffusion time of $\mathbf{M}(t)$ with $\tau_0 = \beta\mu_0 M_S/(2\gamma)$, $\beta = v/(kT)$, v is the volume of a typical particle, k is Boltzmann's constant, and T is the absolute temperature. A general method of solving Eq. (1) and the Fokker-Planck Eq. (2) for *arbitrary* magnetocrystalline anisotropy energy density is given in Ref. 14 (see also Ref. 15,

Chapter 9). We remark that Eq. (2), omitting the second (precessional) term on the right hand side, is essentially similar to the Smoluchowski equation describing dielectric and Kerr effect relaxation in polar liquids.[15] However, the precessional term has a profound effect on the magnetization dynamics especially in the nonlinear case because it may couple, depending on the *direction* of the applied field, the longitudinal and transverse modes in Eq. (1) or (2) as we shall presently see.

Now in the most basic model used to study nonlinear relaxation processes, the free-energy density V of a single-domain nanoparticle with uniaxial anisotropy in superimposed homogeneous external dc bias and ac magnetic fields $\mathbf{H}_0 + \mathbf{H}\cos\omega t$ of arbitrary strengths and orientations relative to the easy axis of the particle is given by

$$\beta V = \sigma \sin^2\vartheta - \xi_0(\mathbf{u}\cdot\mathbf{H}_0)/H_0 - \xi\cos\omega t(\mathbf{u}\cdot\mathbf{H})/H, \quad (3)$$

where $\sigma = \beta K$, $\xi_0 = \beta H_0 M_S$, and $\xi = \beta H M_S$ are the dimensionless anisotropy and external field parameters, and K is the anisotropy constant. Various treatments of the nonlinear ac stationary response have been effected by means of numerical solutions of the governing dynamical Eqs. (1) and/or (2). In particular, efficient numerical algorithms for the calculation of the nonlinear ac stationary response of the magnetization of *uniaxial* magnetic nanoparticles have been proposed[16,17] by assuming that the dc bias and ac driving fields *are directed along the easy axis* of the particle. However, in the *axially symmetric* configuration, many interesting nonlinear effects are suppressed because no dynamical coupling between the longitudinal and transverse precessional modes of motion exists. These mode coupling effects in the *nonlinear* ac stationary response can only be modelled for uniaxial particles driven by a strong ac field applied at *an angle* to the easy axis of the particle so that the axial symmetry is broken by the Zeeman energy.[18–21] Now building on the axially symmetric solutions described in Refs. 16 and 17, an exact nonperturbative method for the determination of the Fourier amplitudes and so the nonlinear magnetization of magnetic nanoparticles with an *arbitrary* anisotropy potential and subjected to a strong ac driving field superimposed on a strong dc bias field has recently been given by Titov *et al.*[22] The method is rooted in posing the solution of the averaged magnetic Langevin Eq. (1) for the statistical moments (expectation values of the spherical harmonics) in terms of matrix continued fractions in the frequency domain (for full details see Ref. 22). So far this method has been used to determine the dynamic susceptibilities (linear, cubic, etc.) and dynamic hysteresis loops in uniaxial magnetic nanoparticles in Refs. 20 and 22. Here, we focus for the first time on nonlinear frequency-dependent effects in the *time-independent* dc component of the magnetization in superimposed external dc bias and ac magnetic fields, which were overlooked in previous studies. Thus we shall demonstrate that under such conditions, the dc magnetization of a magnetic nanoparticle drastically alters leading to pronounced nonlinear effects including three dispersion bands at low, intermediate, and high frequencies in the dc magnetization spectrum. We shall also evaluate the dc magnetization of *an assembly* of noninteracting uniaxial nanoparticles with *randomly* oriented easy axes in space which display similar nonlinear phenomena.

II. BASIC RELATIONS

Henceforth, we shall assume that the easy axis of the particles coincides with the Z axis of the laboratory coordinate system and that $\mathbf{H}_0$ and $\mathbf{H}$ are parallel, lie in the XZ plane and applied at an oblique angle ψ with respect to the Z axis. The method of Titov *et al.*[22] for solving the magnetic Langevin Eq. (1) subjected to ac and dc magnetic fields $\mathbf{H}(t) = \mathbf{H}_0 + \mathbf{H}\cos\omega t$ may be briefly summarized as follows. First, the magnetic Langevin Eq. (1) is transformed to an infinite hierarchy of stochastic differential-recurrence relations for the spherical harmonics $Y_{l,m}(\vartheta,\varphi)$,[23] which on averaging over their realizations in the space of polar angles (ϑ,φ) of $\mathbf{M}$ using the properties of white noise yield deterministic differential-recurrence relations for the statistical moments $\langle Y_{l,m}\rangle(t)$, viz.,

$$\begin{aligned}
&\tau_N \frac{d}{dt}\langle Y_{l,m}\rangle(t) + \left[\frac{l(l+1)}{2} + \frac{im}{2\alpha}(\xi_0 + \xi\cos\omega t)\cos\psi - \sigma\frac{l(l+1)-3m^2}{(2l-1)(2l+3)}\right]\langle Y_{l,m}\rangle(t) \\
&= \frac{\sigma(l+1)}{2l-1}\sqrt{\frac{(l^2-m^2)\left[(l-1)^2-m^2\right]}{(2l-3)(2l+1)}}\langle Y_{l-2,m}\rangle(t) - \frac{\sigma l}{2l+3}\sqrt{\frac{\left[(l+2)^2-m^2\right]\left[(l+1)^2-m^2\right]}{(2l+5)(2l+1)}}\langle Y_{l+2,m}\rangle(t) \\
&+ \left[(\xi_0+\xi\cos\omega t)\frac{l+1}{2}\cos\psi - \frac{im\sigma}{\alpha}\right]\sqrt{\frac{l^2-m^2}{4l^2-1}}\langle Y_{l-1,m}\rangle(t) - \left[(\xi_0+\xi\cos\omega t)\frac{l}{2}\cos\psi + \frac{im\sigma}{\alpha}\right]\sqrt{\frac{(l+1)^2-m^2}{(2l+3)(2l+1)}}\langle Y_{l+1,m}\rangle(t) \\
&- \frac{(\xi_0+\xi\cos\omega t)\sin\psi}{4}\left[\frac{i}{\alpha}\sqrt{(l-m+1)(l+m)}\langle Y_{l,m-1}\rangle(t) - \frac{i}{\alpha}\sqrt{(l+m+1)(l-m)}\langle Y_{l,m+1}\rangle(t)\right. \\
&+ (l+1)\sqrt{\frac{(l+m)(l+m-1)}{4l^2-1}}\langle Y_{l-1,m-1}\rangle(t) + (l+1)\sqrt{\frac{(l-m)(l-m-1)}{4l^2-1}}\langle Y_{l-1,m+1}\rangle(t) \\
&\left. + l\sqrt{\frac{(l-m+1)(l-m+2)}{(2l+3)(2l+1)}}\langle Y_{l+1,m-1}\rangle(t) + l\sqrt{\frac{(l+m+1)(l+m+2)}{(2l+3)(2l+1)}}\langle Y_{l+1,m+1}\rangle(t)\right], \qquad (4)
\end{aligned}$$

where the angular brackets $\langle\ \ \rangle(t)$ denote the ensemble averaging in the presence of the ac field. Then by confining ourselves to the stationary solution for the magnetization in the direction of the ac driving field $m(t) = M_S\langle\cos\Theta\rangle(t)$, where Θ is the angle between the vectors **M** and **H** so that $\cos\Theta = \cos\psi\cos\vartheta + \sin\psi\sin\vartheta\cos\varphi$ and using the known definitions of the spherical harmonics of the first rank, viz.,[23]

$$Y_{1,0} = \sqrt{\frac{3}{4\pi}}\cos\vartheta, \quad Y_{1,\pm1} = \mp\sqrt{\frac{3}{8\pi}}\sin\vartheta e^{\pm i\varphi}, \tag{5}$$

we see that the magnetization $m(t)$ can be expressed via the statistical moments $\langle Y_{1,0}\rangle(t)$ and $\langle Y_{1,\pm1}\rangle(t)$ as

$$m(t) = M_S\sqrt{\frac{2\pi}{3}}\{\sqrt{2}\cos\psi\langle Y_{1,0}\rangle(t) + \sin\psi[\langle Y_{1,-1}\rangle(t) - \langle Y_{1,1}\rangle(t)]\}. \tag{6}$$

Now $m(t)$ must be developed in the Fourier series (because unlike the linear response all harmonics of the driving field will now be involved)

$$m(t) = M_S\sum_{k=-\infty}^{\infty} m_1^k(\omega)\, e^{ik\omega t}, \tag{7}$$

where $m_1^k(\omega)$ is the amplitude of the kth harmonic in the nonlinear response given by[22] [cf. Eq. (8) of that paper]

$$m_1^k(\omega) = \sqrt{\frac{2\pi}{3}}\left\{\sqrt{2}\cos\psi c_{1,0}^k(\omega) + \sin\psi\left[c_{1,-1}^k(\omega) - c_{1,1}^k(\omega)\right]\right\}. \tag{8}$$

The $c_{l,m}^k(\omega)$ are themselves the Fourier coefficients in a Fourier series development in the time of the average spherical harmonics governed by the evolution Eq. (4), viz.,

$$\langle Y_{l,m}\rangle(t) = \sum_{k=-\infty}^{\infty} c_{l,m}^k(\omega)\, e^{ik\omega t}. \tag{9}$$

However, the Fourier coefficients $c_{l,m}^k(\omega)$ of the kth harmonic component in Eq. (9) with $l = 1$ and $m = 0, \pm1$ of the average spherical harmonics $\langle Y_{1,0}\rangle(t)$ and $\langle Y_{1,\pm1}\rangle(t)$ underpinning the magnetization nonlinear response are connected to *all other* Fourier coefficients $c_{l,m}^k(\omega)$ of spherical harmonics of different ranks via the differential-recurrence relation, Eq. (4). Nevertheless, despite this entanglement, the particular coefficients $c_{1,m}^k(\omega)$ pertaining to Eq. (8) can be calculated numerically via matrix continued fractions (details in Ref. 22, particularly Eq. (3) *et seq.*).

Here, we focus on the *time-independent* or dc component of the magnetization $M_\xi(\omega)$ defined by the mean value

$$M_\xi(\omega) = \frac{\omega}{2\pi M_S}\int_0^{2\pi/\omega} m(t)\, dt = m_1^0(\omega), \tag{10}$$

which we note is entirely real. The analysis may be simplified as follows. First, we note that in the limits of *vanishing ac field*, $\xi \to 0$, and/or of *very high frequency field*, $\omega \to \infty$, Eqs. (8) and (10) yield two limiting values for the dc magnetization, which are

$$\lim_{\xi\to0} M_\xi(\omega) = M_0 \text{ and } \lim_{\omega\to\infty} M_\xi(\omega) = M_\xi(\infty),$$

respectively. However, both of the foregoing limits are equal, i.e., $M_\xi(\infty) = M_0 = M_0(\sigma, \xi_0, \psi)$, and can be expressed simply in terms of the stationary average $\langle\cos\Theta\rangle_0$ as

$$M_\xi(\infty) = M_0 = \langle\cos\Theta\rangle_0, \tag{11}$$

where the angular brackets $\langle\ \ \rangle_0$ denote *stationary* ensemble averaging, namely,

$$\langle\cos\Theta\rangle_0 = \frac{1}{Z}\int_0^{2\pi}\int_0^{\pi}\cos\Theta\, e^{\sigma\cos^2\vartheta + \xi_0\cos\Theta}\sin\vartheta d\vartheta d\varphi, \tag{12}$$

$$Z = \int_0^{2\pi}\int_0^{\pi} e^{\sigma\cos^2\vartheta + \xi_0\cos\Theta}\sin\vartheta d\vartheta d\varphi \tag{13}$$

is the partition function. In the opposite *very low frequency* limit, $\omega \to 0$, the mean value $M_\xi(0)$ can also be evaluated by using a quasistatic Boltzmann distribution in Eqs. (12) and (13) as

$$M_\xi(0) = \lim_{\omega\to0}\frac{\omega}{2\pi}\int_0^{2\pi/\omega} M_0(\sigma, \xi_0 + \xi\cos\omega t, \psi)dt. \tag{14}$$

Moreover, the condition $\xi \ll 1$ corresponds to the response to a *weak* ac field so that perturbation theory is valid. Here, the dispersion amplitude $M_\xi(\infty) - M_\xi(0)$ can be evaluated again from Eqs. (12) and (14) via the stationary averages $\langle\cos\Theta\rangle_0$, $\langle\cos^2\Theta\rangle_0$, and $\langle\cos^3\Theta\rangle_0$ as

$$M_\xi(0) - M_\xi(\infty) = \frac{\xi^2}{4}\left(\langle\cos^3\Theta\rangle_0 - 3\langle\cos^2\Theta\rangle_0\langle\cos\Theta\rangle_0 + 2\langle\cos\Theta\rangle_0^3\right) + o\left(\xi^2\right). \tag{15}$$

Furthermore, for axial symmetry, $\psi = 0$, i.e., where both the dc bias and ac fields are applied along the easy axis, we have $\psi = 0$ and $\Theta = \vartheta$, so that Eqs. (11)–(13) become known integrals, viz.,

$$M_0(\sigma, \xi_0, 0) = \langle\cos\vartheta\rangle_0 = \frac{1}{Z}\int_{-1}^{1} xe^{\sigma x^2 + \xi_0 x}dx = \frac{e^\sigma\sinh\xi_0}{\sigma Z} - \frac{\xi_0}{2\sigma}, \tag{16}$$

where the partition function Z is given by

$$Z = \int_{-1}^{1} e^{\sigma x^2 + \xi_0 x}dx = \frac{1}{2}\sqrt{\frac{\pi}{\sigma}}e^{-\frac{\xi_0^2}{4\sigma}}\left\{\mathrm{erfi}\left[\sqrt{\sigma}\left(1 + \frac{\xi_0}{2\sigma}\right)\right] + \mathrm{erfi}\left[\sqrt{\sigma}\left(1 - \frac{\xi_0}{2\sigma}\right)\right]\right\} \tag{17}$$

and

$$\mathrm{erfi}(z) = \frac{2}{\sqrt{\pi}} \int_0^z e^{t^2} dt$$

is the error function of imaginary argument. Hence, in all the foregoing limits, only a knowledge of the equilibrium averages is required.

Now regarding the behavior of $M_\xi(\omega)$ as a function of the ac field amplitude, we remark that strong nonlinear effects in the dc magnetization are expected for $\xi > 1$. For example, for cobalt nanoparticles with mean diameter $a \sim 10$ nm and saturation magnetization $M_S \approx 1.4 \cdot 10^6 \mathrm{A\,m^{-1}}$, the field parameter ξ has order unity for $H \sim 6kT/(\pi a^3 \mu_0 M_S) \sim 4.5 \cdot 10^3$ A m^{-1} for $T \sim 30$ K. Moreover, an ac field of this order of magnitude is easily attainable in practical measurements of the nonlinear response of magnetic nanoparticles.[4] On the other hand, the condition $\xi \ll 1$ corresponds to the response to a weak ac field, where we have stated that perturbation theory is valid. Here, because the nonlinear contribution to the dc magnetization has order ξ^2, $M_\xi(\omega)$ is itself only weakly dependent upon ξ nevertheless it strongly depends on the angle ψ, dc bias field ξ_0, and anisotropy parameter σ.

III. DC MAGNETIZATION FOR $\psi = 0$

In order to illustrate the nonlinear effects in the time-independent but frequency-dependent magnetization $M_\xi(\omega)$ induced by the ac field, which in general exhibits a pronounced frequency dependence due to the ac field acting in conjunction with the bias field, we plot $M_\xi(\omega)$ as a function of the dc field, frequency, and inverse temperature for various ac field magnitudes ξ, damping α, and lastly oblique angle ψ between the bias field and easy axis.

We first present results for the dc magnetization of an assembly of *aligned* nanoparticles with the angle $\psi = 0$ so that axial symmetry prevails. Then in the small ac field limit, $\xi \ll 1$, the dc component $M_\xi(\omega)$ can be evaluated analytically via perturbation theory (see below) while in strong ac driving fields, $\xi > 1$, $M_\xi(\omega)$ can be determined using the matrix continued fraction method as applied to axially symmetric problems.[17] To facilitate our discussion, plots of both $M_\xi(\omega)$ and the real part of the *fundamental* component, i.e., the term prefixed by $e^{i\omega t}$ in Eq. (7), of the nonlinear dynamic susceptibility $\chi(\omega) = 2m_1^1/\xi$ (Ref. 15) as a function of the normalized frequency $\omega\,\tau_N$ for various values of the anisotropy (or inverse temperature) parameter $\sigma = vK/(kT)$ are shown in Fig. 1. By inspection of that figure, two distinct low- and high-frequency dispersion bands appear in the spectrum of $M_\xi(\omega)$ just as with the susceptibility $\chi(\omega)$ (in the latter the second dispersion region would be visible on the logarithmic scale[15,17]). Moreover, the low-frequency dispersion of each of the two functions $M_\xi(\omega)$ and $\chi(\omega)$ clearly are governed by barrier crossing relaxation modes with the *same* characteristic frequency *indicating that the magnetization reversal time may be directly determined from measurements of the dc response* $M_\xi(\omega)$. In addition, for weak ac fields, the

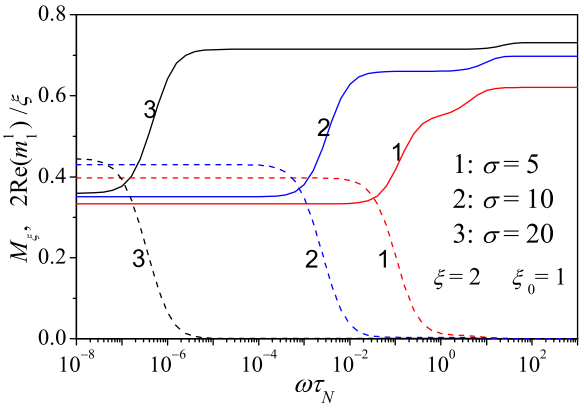

FIG. 1. Comparison of the dc magnetization M_ξ (solid lines) and real part of the fundamental component of the nonlinear dynamic susceptibility $2\mathrm{Re}(m_1^1)/\xi$ (dashed lines) vs. normalized frequency $\omega\,\tau_N$ for $\xi_0 = 1$, $\xi = 2$, $\alpha = 1$, and various anisotropy parameter $\sigma = vK/(kT)$.

characteristic frequency ω_1 of this low-frequency band may be determined explicitly as $\omega_1 = \lambda_1$ via the smallest nonvanishing eigenvalue λ_1 of the Fokker-Planck operator in Eq. (2) associated with the overbarrier relaxation processes. We recall that subject to $\xi \ll 1$, λ_1 for the potential of Eq. (3) with $\psi = 0$, corresponding to axial symmetry, is given by Brown's formula[13]

$$\lambda_1 \sim \frac{(1-h^2)\sqrt{\sigma^3}}{\tau_N \sqrt{\pi}} \left[(1+h) e^{-\sigma(1+h)^2} + (1-h) e^{-\sigma(1-h)^2} \right], \quad (18)$$

where $h = \xi_0/(2\sigma) = \mu_0 M_S H_0/(2K)$. Equation (18) because it relates to an axially symmetric system governed by a scalar differential-recurrence relation for the observables in the time domain is valid for all values of the damping α. Now for cobalt nanoparticles with anisotropy constant $K \sim 10^5$ J/m^3 and $\alpha \sim 0.1$, the free diffusion relaxation time is $\tau_N \sim 4 \cdot 10^{-10}$ s (with $\gamma = 2.2 \cdot 10^5$ m A^{-1} s^{-1}). Furthermore, via the critical value[15] of the dimensionless parameter $h = \mu_0 M_S H_0/(2K) = 1$ at which the double well structure of the magnetocrystalline/Zeeman energy $\sigma \sin^2\vartheta - \xi_0 \cos\Theta$ disappears, one may infer that the low-frequency overbarrier relaxation processes vanish for a dc bias field $H_0 \approx 1.14 \cdot 10^5$ A m^{-1}. Now at the opposite end of the spectrum, the high-frequency band is due to "intrawell" relaxation modes. These individual near-degenerate high frequency modes are, however, virtually indistinguishable in the frequency spectrum of $M_\xi(\omega)$ appearing merely as a single high-frequency dispersion again as in the dynamic susceptibility. Thus, like the latter,[15] the spectrum of $M_\xi(\omega)$ may in practice be approximated by a sum of two Lorentzians, viz.,

$$M_\xi(\omega) \approx M_\xi(\infty) + \left[M_\xi(0) - M_\xi(\infty) \right] \times \left(\frac{\Delta}{1 + (\omega/\omega_1)^2} + \frac{1-\Delta}{1 + (\omega/\omega_2)^2} \right). \quad (19)$$

Here, ω_1 and ω_2 are, respectively, the characteristic frequencies of the overbarrier relaxation modes which are related to the Kramers escape rate $\Gamma \sim \lambda_1$ and the near-degenerate high frequency "intrawell" relaxation modes (both in the

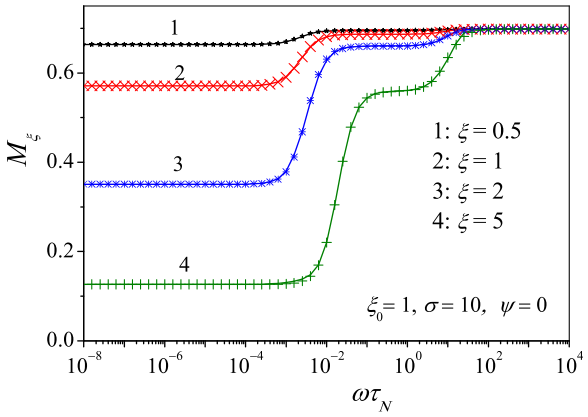

FIG. 2. Dc magnetization M_ξ vs. normalized frequency $\omega\tau_N$ for $\sigma = 10$, $\xi_0 = 1$, and various values of the ac field amplitude ξ showing pronounced frequency-dependence including two distinct dispersion regions caused by entanglement of the dc and ac responses. Solid lines: exact matrix continued fraction solution. Symbols: the approximate fitting Eq. (19).

presence of an ac external field), and Δ is an adjustable amplitude parameter.

The dc magnetization $M_\xi(\omega)$ obtained via the matrix continued fraction method[15] as a function of the normalized frequency $\omega\tau_N$ and as a function of the dc field ξ_0 for various values of the ac driving field amplitude ξ is shown in Figs. 2 and 3, respectively. Furthermore, M_ξ as a function of the inverse temperature parameter σ for the particular dc field amplitude $\xi_0 = 1$ is shown in Fig. 4. As shown in Figs. 2–4, the approximate Eq. (19) above accurately fits the numerical matrix continued fraction results. The corresponding fitting parameters ω_1, ω_2, and Δ as functions of ac field amplitude ξ are exhibited in Fig. 5. In Figs. 1 and 2, the limiting values of $M_\xi(\omega)$ as $\omega \to \infty$ and as $\omega \to 0$ are, respectively, $M_\xi(\infty) = M_0(\sigma, \xi_0, 0)$ from Eq. (16) and $M_\xi(0)$ from Eq. (14) with $\psi = 0$. We remark that for weak ac fields $\xi \ll 1$ and $\sigma(1-h)^2 \gg 1$, ω_1 can be evaluated explicitly from Brown's asymptotic lowest nonvanishing eigenvalue expression Eq. (18) as then $\omega_1 = \lambda_1$. Furthermore, for both

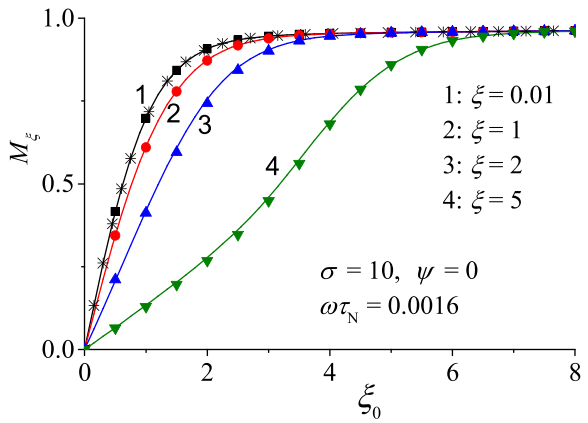

FIG. 3. Dc magnetization M_ξ vs. dc field $\xi_0 = vM_SH_0/(kT)$ for $\omega\tau_N = 0.0016$, $\sigma = 10$, and various values of the ac field ξ ($\xi = 0.01$ represents linear response conditions where the ac and dc field responses do not entangle). Solid lines: exact matrix continued fraction solution. Asterisks: the weak field solution rendered by Eq. (16). Symbols: the approximate Eq. (19). All curves display more or less monotonic increase to the asymptotic value.

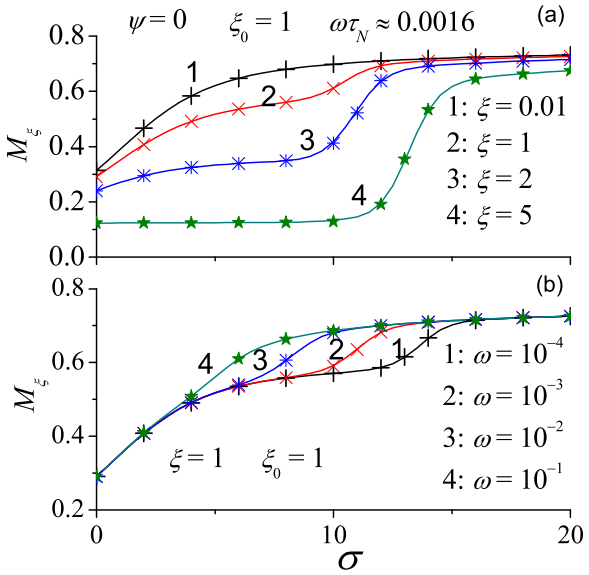

FIG. 4. Dc magnetization M_ξ vs. inverse temperature parameter $\sigma = vK/(kT)$ for dc parameter $\xi_0 = 1$, and for various values of the ac parameter ξ at $\omega\tau_N = 0.0016$ (a) and for various ω at $\xi = 1$ (b). Solid lines: exact matrix continued fraction solution. Symbols: the approximate fitting Eq. (19). Notice the pronounced field and frequency dependence.

$\xi, \xi_0 \ll 1$ with $\sigma = 0$, i.e., zero anisotropy, the approximate Eq. (19) concurs with the known perturbation solution of the Fokker-Planck Eq. (2) for axial symmetry,[24] namely,

$$M_\xi(\omega) = \frac{\xi_0}{3} - \frac{\xi_0^3}{45} - \frac{\xi_0\xi^2}{180}\left(\frac{5}{1+\omega^2\tau_N^2} + \frac{1}{1+\omega^2\tau_N^2/9}\right) + \dots . \tag{20}$$

Here, the first two terms on the right hand side constitute the expansion of the Langevin function in the dc field alone while the last term refers to the combined effect of the strong dc and ac fields. Moreover, now $\omega_1 = \tau_N^{-1}$, where the free diffusion time τ_N is a characteristic time of the first rank relaxation function $\langle Y_{1,0}\rangle(t)$ while the frequency $\omega_2 = (3\tau_N)^{-1}$ characterizes the contribution of the second rank relaxation function $\langle Y_{2,0}\rangle(t)$ to the dc magnetization.

IV. DC MAGNETIZATION FOR $\psi \neq 0$

The results so far pertain to both dc bias and ac fields applied *parallel* to the easy axis of a uniaxial particle. Thus the inherent coupling between the longitudinal relaxational and transverse precessional modes implied by the magnetic Langevin Eq. (1) is automatically suppressed due to axial symmetry, where the orders $m \neq 0$ of the spherical harmonics are not involved. Hence the important precessional and mode coupling effects which are present in nonaxially symmetric potentials cannot be detected if one is so restricted. If, in contrast, the external fields are applied at an oblique angle ψ to the easy axis so breaking the axial symmetry (meaning that the differential-recurrence relation Eq. (4) involves averages of spherical harmonics of different orders m besides those of different rank l) pronounced precessional and longitudinal mode coupling effects will occur in the frequency-dependent dc magnetization. These nonlinear frequency-dependent

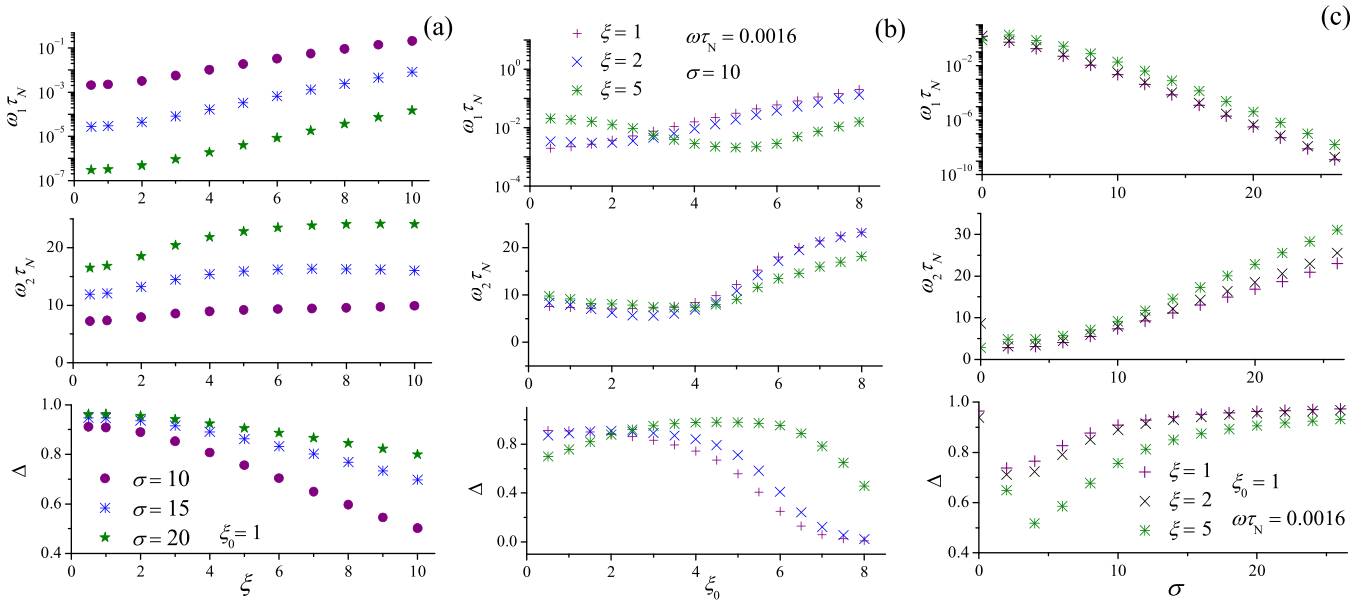

FIG. 5. Characteristic fitting parameters ω_1, ω_2, and Δ vs. (a) the ac field parameter ξ, (b) the dc field parameter ξ_0, and (c) the inverse temperature parameter σ. These parameter values were used in Figs. 2–4.

effects due to the loss of axial symmetry principally comprise a new high-frequency dispersion of resonant character in the vicinity of the frequency ω_{pr} of the ferromagnetic resonance (FMR), which also exhibits parametric resonance (see Fig. 6) and angular dependence of the dc magnetization curves (see Fig. 7). Both effects arise from the coupling inherent in Eq. (4) of the slow thermally activated magnetization reversal mode with the fast precessional modes via the driving ac field acting in conjunction with the dc bias field.

The high-frequency resonance dispersion in the spectrum of $M_\xi(\omega)$ originating in excitation of transverse modes having frequencies close to the precession frequency ω_{pr} of the magnetization appears only at low damping and $\psi \neq 0$, i.e., when the axial symmetry is broken. In contrast for axial symmetry $\psi = 0$, the high-frequency dispersion disappears

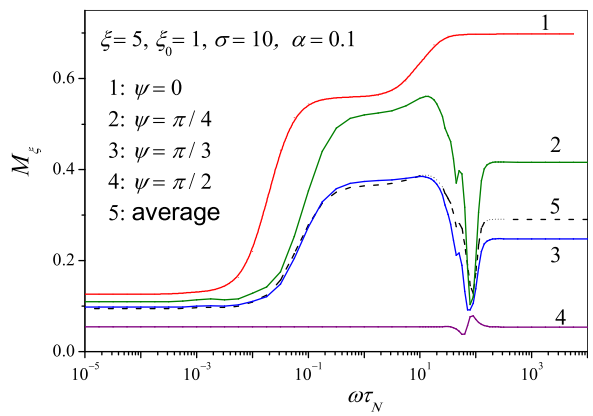

FIG. 6. Dc magnetization M_ξ vs. normalized frequency $\omega\tau_N$ for $\sigma = 10$, $\xi_0 = 1$, $\xi = 5$, and various values of the oblique angle ψ between the bias field and easy axis showing pronounced frequency dependence now comprising three distinct dispersion regions. Solid lines (1–4): exact matrix continued fraction solution. Dashed line 5: the average dc magnetization $\bar{M}_\xi$ from Eq. (22) below. Notice the much weaker effect for a purely transverse applied field $\psi = \pi/2$.

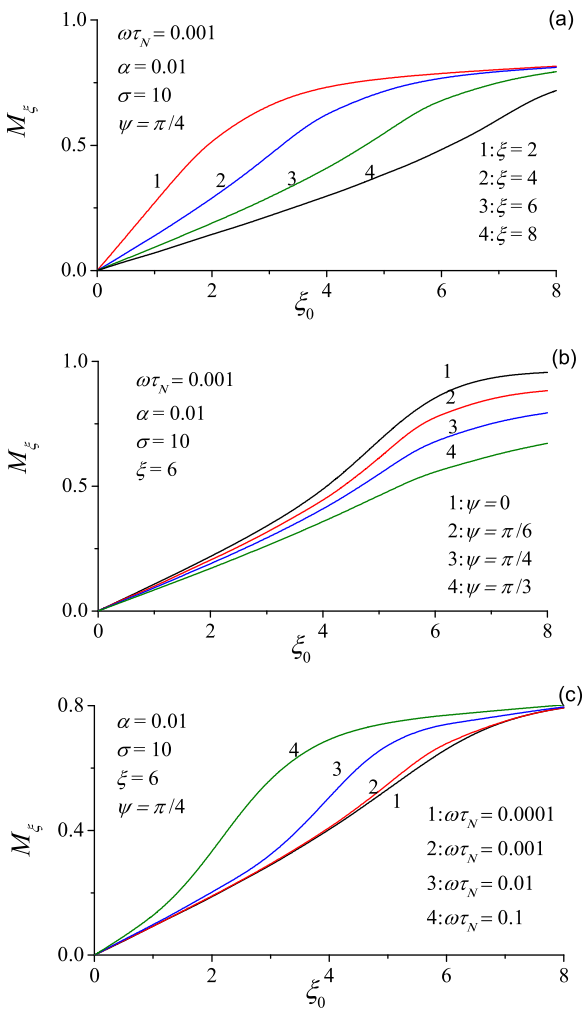

FIG. 7. M_ξ vs. normalized dc field $\xi_0 = vM_SH_0/(kT)$ for various ac field amplitudes ξ (a), oblique angles ψ (b), and frequency ω (c).

altogether because the transverse modes no longer take part in the relaxation process [see Fig. 6 and Eq. (4) above]. Furthermore, just as with the nonlinear dynamic susceptibility for low damping,[22] a subharmonic weak resonance dispersion owing to parametric resonance of the nonlinear oscillatory (precessional) motion of the magnetization $\mathbf{M}(t)$ appears at frequencies $\sim\omega_{pr}/2$ (Fig. 6). In Fig. 6, the limiting values of $M_\xi(\omega)$ as $\omega \to 0$ and as $\omega \to \infty$ are given by Eqs. (12) and (14), respectively. Notice that the appearance of a high-frequency dispersion region of resonant character is entirely consistent with the concept[15] of the role of coupling between transverse and longitudinal modes in the magnetization problem as being in certain ways analogous to that played by inertia in mechanical problems with separable and additive Hamiltonians.[25] For example, in the escape rate problem for both mechanical and magnetic systems, the role of inertia and mode-coupling respectively is to give rise to the limiting cases of spatially and energy-controlled diffusion identified by Kramers[26] with a turnover region between them.[27] This is true regardless of the fact that the physical origin of the various diffusion regimes is in each case entirely different. In the magnetic situation, the diffusion regimes spring from the lack of axial symmetry and so are geometric in origin while in the mechanical one they stem from including the inertia of the particles. However, the common feature that unites the two systems is that very similar differential-recurrence relations in the time domain are involved in both. For example, in the magnetic case, the recurrence relation is in the recurring numbers l and m of the spherical harmonics; while in the mechanical case, the recurrence relation is in the order n of the orthogonal Hermite polynomials describing the variation of the phase space density function with momentum while the second recurring number m is that associated with the variation of the phase space density function with position.

For the oblique field configuration again, just as with $\psi = 0$, the low-frequency dispersion of $M_\xi(\omega)$ is governed by slow barrier crossing relaxation modes with the characteristic frequency ω_1. Therefore, for relatively weak ac driving fields, $\xi \ll 1$, ω_1 may again be associated with the smallest nonvanishing eigenvalue λ_1 for the potential given by Eq. (3) with $\xi = 0$ as $\omega_1 = \lambda_1$. Now the high barrier (or low temperature) asymptote for λ_1 for nonaxially symmetric potentials valid for all damping regimes has been obtained by Coffey *et al.*[25] This was accomplished by extending the Kramers theory,[26] as generalized by Mel'nikov and Meshkov,[27] of thermally activated escape of point particles over a potential barrier to the magnetization reversal so as to include the turnover region between the transition state theory and the very low damping or energy-controlled diffusion regime (see Ref. 28 for a review of application of the Kramers theory to magnetic nanoparticles). Therefore, since in the weak ac field case, we are effectively treating a *nonaxially symmetric* double-well potential with *nonequivalent* wells as is evident from Eq. (3), λ_1 is formally given by[29]

$$\lambda_1(\sigma, \alpha, \xi_0, \psi) \sim \left(\Gamma_1^{IHD} + \Gamma_2^{IHD}\right) \frac{A(\alpha S_1)A(\alpha S_2)}{A(\alpha S_1 + \alpha S_2)}. \qquad (21)$$

A result which despite being *formally* similar to that for point particles is rooted in the lack of axial symmetry rather than in inertial effects. Here, $A(\delta)$ and S_i are, respectively, the depopulation factor and the actions calculated at the saddle point of the ith well, $\Gamma_i^{IHD} = \Omega_0\omega_i e^{-\Delta V_i}/(2\pi\omega_0)$ are the Kramers escape rates in the so-called intermediate-to-high damping (IHD) limit, where ΔV_i is the dimensionless barrier height, ω_i and ω_0 are the well and saddle angular frequencies respectively, and Ω_0 is the damped saddle angular frequency. Explicit equations for all quantities appearing in the asymptotic smallest nonvanishing eigenvalue Eq. (21) are given in Refs. 28 and 29. The simple analytic Eq. (21) then allows one to accurately estimate[15] the damping dependence of the relaxation time of the magnetization for values of the angle ψ and the field parameter $h = \xi_0/(2\sigma)$ such that $h \sin\psi > 0.03$ and $h < h_c(\psi) = (\cos^{2/3}\psi + \sin^{2/3}\psi)^{-3/2}$.

V. DC MAGNETIZATION FOR ASSEMBLIES

All the previous frequency-dependent nonlinear dc response results concern either a *single* particle or an assembly of noninteracting particles with *aligned* easy axes. However, we can also calculate the dc magnetization $\overline{M_\xi}$ of an assembly of noninteracting uniaxial particles with *randomly* oriented easy axes, where the overbar denotes averaging over the angle ψ. Averaging over particle easy axis orientations can be accomplished numerically. In the calculation of $\overline{M_\xi}$ for randomly oriented easy axes using Gaussian quadratures,[23] we only require[23]

$$\overline{M_\xi} = \int_0^{\pi/2} m_1^0(\omega, \psi)\sin\psi d\psi = \frac{\pi}{4}\sum_{i=1}^{n} w_i m_1^0(\omega, \psi_i)\sin\psi_i, \quad (22)$$

where

$$w_i = \frac{2\left(1 - x_i^2\right)}{\left[(n+1)P_{n+1}(x_i)\right]^2}, \quad \psi_i = \frac{\pi}{4}(x_i + 1),$$

and x_i is the ith root of the Legendre polynomial $P_n(x)$ [here, we have noted that $m_1^0(\psi) = m_1^0(\pi - \psi)$] and the usual recursion relations for the Legendre polynomials[23] have been used.

First of all referring to Fig. 6 alone, $\overline{M_\xi}$ as a function of the normalized frequency $\omega\tau_N$ for an assembly of noninteracting uniaxial particles with randomly oriented easy axes is compared with M_ξ for an individual particle for the particular values $\psi = 0$, $\pi/6$, $\pi/4$, and $\pi/2$. Here, three distinct dispersion bands again appear in the spectrum of $\overline{M_\xi}$ just as with the average dynamic susceptibility.[15,17] Next, plots of $\overline{M_\xi}$ as a function of $\omega\tau_N$ for various values of the ac driving field amplitude ξ as parameter are shown in Fig. 8. As seen in Fig. 8, with increasing ξ, the magnitude of the dispersion in the vicinity of the precession frequency ω_{pr} increases showing pronounced nonlinear effects including parametric resonance. Furthermore, for a given value of ξ, the nonlinear response strongly depends on the angle ψ, dc bias field ξ_0, barrier height σ, and damping α.

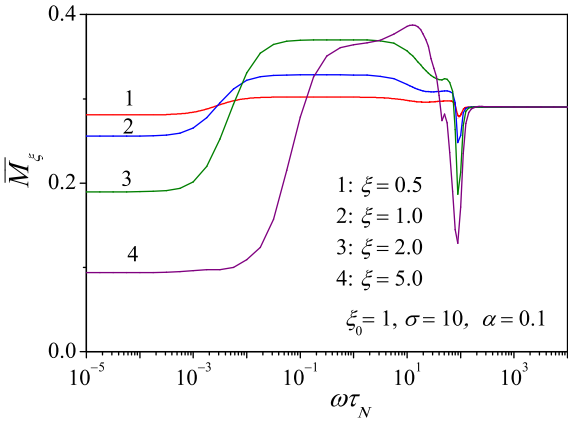

FIG. 8. Average dc magnetization $\bar{M}_\xi$ vs. normalized frequency $\omega\tau_N$ for $\sigma = 10$, $\alpha = 0.1$, $\xi_0 = 1$, and various values of the ac field amplitude ξ. Notice the parametric resonance behavior in the high frequency dispersion in curve 4 (a subharmonic weak resonance dispersion at frequencies $\sim\omega_{pr}/2$).

VI. CONCLUSIONS

We have treated the time-independent but frequency-dependent magnetization for an ensemble of fully aligned noninteracting particles, as well as that of an ensemble of particles with randomly oriented easy axes, driven by strong dc and ac fields using a nonperturbative approach. We have shown owing to the coupling between the fast precession of the magnetization and its slow thermally activated reversal that the *average* magnetization (with a strong ac field applied in conjunction with a strong dc bias field at an angle to the easy axis of the particle so that the axial symmetry is broken) is very sensitive to both ac field orientation, amplitude, and frequency. The influence of field orientation and magnitude seems particularly obvious in retrospect by inspection of the equation of motion of an average spherical harmonic explicitly in the time domain, Eq. (4). All our calculations, since they are valid for ac fields of arbitrary strengths and orientations, allow one to predict and interpret quantitatively nonlinear phenomena in magnetic nanoparticles, where perturbation theory and the assumption that axial symmetry is preserved are no longer valid. In general, from a theoretical point of view, the nonlinear behavior of the *frequency-dependent* dc component of the magnetization of nanomagnets driven by an ac external magnetic field closely resembles both that of the frequency-dependent dc component of the dynamic Kerr effect in both polar liquids and liquid crystals[30,31] insofar as it has a *frequency-dependent* dc response. The results we have obtained suggest that the existing experimental measurements of nonlinear susceptibilities of fine particles, e.g., Refs. 4–6, should be repeated for the frequency-dependent dc component of the magnetization in a strong bias-field configuration showing pronounced nonlinear effects which were overlooked in previous measurements. We also remark that similar nonlinear effects can be measured in the dc polarization of polar liquids in superimposed external dc bias and ac electric fields because from a physical point of view, the stochastic magnetization dynamics of single-domain ferromagnetic particles (magnetic dipoles) in magnetic fields is analogous to the rotational Brownian motion of polar molecules (electric dipoles) in electric fields.[15]

For simplicity, only uniaxial particles have been treated. Particles with non-axially symmetric anisotropies (cubic, biaxial, etc.) can be considered in like manner. We have assumed throughout that all the particles are identical and that interparticle interactions are negligible. In order to account for polydispersity, it is necessary to average over the appropriate distribution function, e.g., over the particle volumes, cf. Ref. 3. The neglect of interparticle interactions in the present model suggests that the results apply only to systems, where interparticle interactions are ignored, such as individual nanoparticles and dilute solid suspensions of nanoparticles.

ACKNOWLEDGMENTS

We would like to thank FP7-PEOPLE-Marie Curie Actions—International Research Staff Exchange Scheme (Project No. 295196 DMH) for financial support. Moreover, W. T. Coffey and N. Wei thank Ambassade de France en Irlande for research visits to Perpignan. N. Wei also acknowledges the Government of Ireland Scholarship Award. D. Byrne acknowledges the SimSci Structured Ph.D. Program at University College Dublin for financial support. SimSci is funded under the Program for Research in Third-level Institutions and cofunded under the European Regional Development Fund. We thank P. Fannin and P. M. Déjardin for helpful conversations. The graphical calculations were carried out using Armadillo: An Open Source C++ Linear Algebra Library for Fast Prototyping and Computationally Intensive Experiments. Technical Report, NICTA, 2010.by Conrad Sanderson.

[1]C. D. Mee, *The Physics of Magnetic Recording* (North Holland, Amsterdam, 1986); A. P. Guimarães, *Principles of Nanomagnetism* (Springer, Berlin, 2009).
[2]Q. A. Pankhurst, N. K. T. Thanh, S. K. Jones, and J. Dobson, J. Phys. D: Appl. Phys. **42**, 224001 (2009); *Magnetic Nanoparticles* edited by S. P. Gubin (Wiley, New York, 2009); D. G. Rancourt, in *Nanoparticles and the Environment, Rev. Mineralogy Geochem.* edited by J. F. Banfield and A. Vavrotsky (2001), Vol. 44, p. 217.
[3]Yu. L. Raikher and V. I. Stepanov, Adv. Chem. Phys. **129**, 419 (2004).
[4]T. Bitoh, K. Ohba, M. Takamatsu, T. Shirane, and S. Chikazawa, J. Phys. Soc. Jpn. **64**, 1311 (1995); J. Magn. Magn. Mater. **154**, 59 (1996).
[5]P. E. Jonsson, T. Jonsson, J. L. García-Palacios, and P. Svedlindh, J. Magn. Magn. Mater. **222**, 219 (2000); L. Spinu, D. Fiorani, H. Srikanth, F. Lucari, F. D'Orazio, E. Tronc, and M. Nogués, J. Magn. Magn. Mater. **226–230**, 1927 (2001); P. E. Jonsson, Adv. Chem. Phys. **128**, 191 (2004).
[6]T. Suneetha, S. C. Kundu, Kashyap, H. C. Gupta, and T. K. Nath, J. Nanosci. Nanotechnol. **13**, 270 (2013).
[7]Yu. L. Raikher, V. I. Stepanov, A. N. Grigorenko, and P. I. Nikitin, Phys. Rev. E **56**, 6400 (1997); Yu. L. Raikher and V. I. Stepanov, Phys. Rev. Lett. **86**, 1923 (2001).
[8]V. A. Ignatchenko and R. S. Gekht, Sov. Phys. JETP **40**, 750 (1975).
[9]J. J. Lu, H. L. Huang, and I. Klik, J. Appl. Phys. **76**, 1726 (1994); I. Klik and Y. D. Yao, *ibid.* **89**, 7457 (2001).
[10]Yu. L. Raikher, V. I. Stepanov, and R. Perzynski, Physica B **343**, 262 (2004); P. M. Déjardin, Yu. P. Kalmykov, B. E. Kashevsky, H. El Mrabti, I. S. Poperechny, Yu. L. Raikher, and S. V. Titov, J. Appl. Phys. **107**, 073914 (2010).
[11]A. Sukhov and J. Berakdar, J. Phys.: Condens. Matter **20**, 125226 (2008).
[12]G. Bertotti, I. Mayergoyz, C. Serpico, M. d'Aquino, and R. Bonin, J. Appl. Phys. **105**, 07B712 (2009).

[13]W. F. Brown, Jr., Phys. Rev. **130**, 1677 (1963); IEEE Trans. Mag. **15**, 1196 (1979).
[14]Yu. P. Kalmykov and S. V. Titov, Phys. Rev. Lett. **82**, 2967 (1999); J. Magn. Magn. Mater. **210**, 233 (2000).
[15]W. T. Coffey and Yu. P. Kalmykov, *The Langevin Equation* 3rd ed. (World Scientific, Singapore, 2012).
[16]Yu. L. Raikher, V. I. Stepanov, and P. C. Fannin, J. Magn. Magn. Mater. **258–259**, 369 (2003); Yu. L. Raikher and V. I. Stepanov, J. Magn. Magn. Mater. **300**, e311 (2006).
[17]P. M. Déjardin and Yu. P. Kalmykov, J. Appl. Phys. **106**, 123908 (2009).
[18]J. L. García-Palacios and P. Svendlindh, Phys. Rev. Lett. **85**, 3724 (2000).
[19]I. S. Poperechny, Yu. L. Raikher, and V. I. Stepanov, Phys. Rev. B **82**, 174423 (2010).
[20]H. El Mrabti, S. V. Titov, P. M. Déjardin, and Yu. P. Kalmykov, J. Appl. Phys. **110**, 023901 (2011), H. El Mrabti, P. M. Déjardin, S. V. Titov, and Yu. P. Kalmykov, Phys. Rev. B **85**, 094425 (2012).
[21]G. T. Landi, J. Magn. Magn. Mater. **324**, 466 (2012); J. Appl. Phys. **111**, 043901 (2012).
[22]S. V. Titov, P. M. Déjardin, H. El Mrabti, and Yu. P. Kalmykov, Phys. Rev. B **82**, 100413(R) (2010).
[23]D. A. Varshalovich, A. N. Moskalev, and V. K. Khersonskii, *Quantum Theory of Angular Momentum* (World Scientific, Singapore, 1998).
[24]W. T. Coffey, Yu. P. Kalmykov, and N. Wei, "Nonlinear normal and anomalous response of non-interacting electric and magnetic dipoles subjected to strong AC and DC bias fields," Nonlinear Dynamics (published online).
[25]W. T. Coffey, D. A. Garanin, and D. J. McCarthy, Adv. Chem. Phys. **117**, 483 (2001); P. M. Déjardin, D. S. F. Crothers, W. T. Coffey, and D. J. McCarthy, Phys. Rev. E. **63**, 021102 (2001).
[26]H. A. Kramers, Physica **7**, 284 (1940).
[27]V. I. Mel'nikov and S. V. Meshkov, J. Chem. Phys. **85**, 1018 (1986); V. I. Mel'nikov, Physica A **130**, 606 (1985); Phys. Rep. **209**, 1 (1991).
[28]W. T. Coffey and Yu. P. Kalmykov, J. Appl. Phys. **112**, 121301 (2012).
[29]Yu. P. Kalmykov, J. Appl. Phys. **96**, 1138 (2004).
[30]G. B. Thurston and D. L. Bowling, J. Coll. Interface Sci. **30**, 34 (1969); K. Hosokawa, T. Shimomura, H. Furusawa, Y. Kimura, K. Ito, and R. Hayakawa, J. Chem. Phys. **110**, 4101 (1999).
[31]H. Watanabe and A. Morita, Adv. Chem. Phys. **56**, 255 (1984); J. L. Déjardin, Yu. P. Kalmykov, and P. M. Déjardin, *ibid.* **117**, 275 (2001); J. L. Déjardin and Yu. P. Kalmykov, Phys. Rev. E **61**, 1211 (2000); J. L. Déjardin and Yu. P. Kalmykov, J. Chem. Phys. **112**, 2916 (2000); W. T. Coffey, D. S. F. Crothers, Yu. P. Kalmykov, and P. M. Déjardin, Phys. Rev. E **71**, 062102 (2005); W. T. Coffey, D. S. F. Crothers, and Yu. P. Kalmykov, J. Non-Crystall. Solids **352**, 4710 (2006).